Stereoisomeric C5−C5′-Linked Dihydrothymine Dimers Produced by Radiolytic One-Electron Reduction of Thymine Derivatives in Anoxic Aqueous Solution: Structural Characteristics in Reference to Cyclobutane Photodimers

Takeo Ito, Hideki Shinohara, Hiroshi Hatta, and Sei-ichi Nishimoto*

Department of Energy and Hydrocarbon Chemistry, Graduate School of Engineering, Kyoto University, Sakyo-ku, Kyoto 606-8501, Japan

Received January 12, 1999

Radiolytic one-electron reduction of 1-methylthymine (**1a**) and 1,3-dimethylthymine (**1b**) in anoxic aqueous solution afforded stereoisomeric C5−C5′-linked dihydrothymine dimers, fractionated into the meso forms of (5*R*,5′*S*)- and (5*S*,5′*R*)-bi-5,6-dihydrothymine (**3a**,**b**[***meso***]) and a racemic mixture of (5*R*,5′*R*)- and (5*S*,5′*S*)-bi-5,6-dihydrothymines (**3a**,**b**[***rac***]), along with 5,6-dihydrothymines (**2a**,**b**). The meso and racemic dimers were produced in almost equivalent yields, possessing structural similarity with *cis-syn*-cyclobutane pyrimidine photodimers that are identified as highly mutagenic and carcinogenic photolesions induced by UV light. Similar radiolytic one-electron reduction of thymidine (**1c**) resulted in the pseudo-meso form of (5*R*,5′*S*)- and (5*S*,5′*R*)-bi-5,6-dihydrothymidine (**3c**[***RS***]) and two diastereormers of (5*R*,5′*R*)- and (5*S*,5′*S*)-bi-5,6-dihydrothymidine (**3c**[***RR***] and **3c**[***SS***]). X-ray crystal structures indicated that two pyrimidine rings of the stereoisomeric dimers except **3a**[***rac***] overlap with each other to a considerable extent, as in the *cis-syn*-cyclobutane photodimers. The pyrimidine rings of the dimers were twisted around 5-Me−C5−C5′−5′-Me by 51.1(2)° for **3a**[***meso***], −85.4(4)° for **3a**[***rac***], −65(1)° for **3b**[***meso***], 43(2)° for **3b**[***rac***], and 64.9(4)° for **3c**[***RS***], respectively. It was predicted that the C5−C5′-linked dihydrothymine dimers may cause some distortion within a DNA duplex if they were incorporated. The pH dependence of the reactivities was in accord with a mechanism of the C5−C5′-linked dimerization by which electron adducts of **1a**−**c** are irreversibly protonated at C6 and the resulting 5,6-dihydrothymin-5-yl radicals undergo bimolecular coupling.

Introduction

Interaction of ionizing radiation with living cells generates excess free radicals to induce a variety of damages to cellular DNA that are responsible for carcinogenic, mutagenic, and lethal effects on the cells.[1] The primary biological effects of ionizing radiation, eventually triggering off the obvious lesions via a sequence of chemical reactions and biological responses on a wide range of time scales, are conventionally classified into two subgroups: the *indirect effect* and *direct effect*.[1a] The indirect effect is attributable largely to hydroxyl radicals (•OH), hydrated electrons (e_{aq}^-), and hydrogen atoms (•H) produced by the radiolysis of excess cellular water (reactions 1 and 3). The direct effect involves absorption of radiation energy by DNA molecule itself to undergo electron ejection into DNA radical cation ($DNA^{\bullet+}$), as is of essential importance upon exposure to high-linear energy transfer (LET) radiation (reaction 2).[2] The concomitant electron ejected from DNA is also hydrated as in reaction 3.

$$H_2O \rightarrow {}^{\bullet}OH + e^- + {}^{\bullet}H \quad (1)$$

$$DNA \rightarrow DNA^{\bullet+} + e^- \quad (2)$$

$$e^- + nH_2O \rightarrow e_{aq}^- \quad (3)$$

Oxidative DNA damages including various base modifications by OH radicals have been extensively studied to elucidate the detailed mechanism of oxidation.[1] Similar oxidative damages may arise from the DNA radical cations induced by the direct effect of radiations. A recent study has shown that an electron-loss center (hole) at a given DNA base radical cation can migrate intramolecularly through a π-stacking of DNA bases, thus arriving at and being trapped most efficiently in a guanine (G) moiety to cause its oxidative damage.[3] Under oxic conditions in the presence of oxygen, these oxidative damages are significantly enhanced, while a reducing species of hydrated electron (e_{aq}^-) is scavenged by oxygen into less reactive superoxide radical ion ($O_2^{\bullet-}$).[1a] Several structures of oxidative DNA-base modifications, particularly those of purine modifications, have been identified to account for the biological lesions.[4]

Concerning reductive DNA damages by dry electrons (e^- as in reactions 1 and 2) and/or hydrated electrons e_{aq}^- (reaction 3), the cytosine base moiety is a major site of

(1) (a) von Sonntag, C. In *The Chemical Basis of Radiation Biology*; Taylor and Francis: London, 1987. (b) Steenken, S. *Free Rad. Res. Commun.* **1992**, *16*, 349−379. (c) von Sonntag, C.; Schuchmann, H.-P. *Int. J. Radiat. Biol.* **1986**, *49*, 1−34. (d) Bensasson, R. V.; Land, E. J.; Truscott, T. G. In *Excited States and Free Radicals in Biology and Medicine*; Oxford University Press: Oxford, 1993; pp 290−305.

(2) Roots, R.; Chatterjee, A.; Chang, P.; Lommel, L.; Blakely, E. A. *Int. J. Radiat. Biol.* **1985**, *47*, 157−166.

(3) (a) Hall, D. B., Holmlin, R. E., Barton, J. K. *Nature* **1996**, *382*, 731−735. (b) Gasper, S. M.; Schuster, G. B. *J. Am. Chem. Soc.* **1997**, *119*, 12762−12771.

(4) (a) Shibutani, S.; Takeshita, M.; Grollmann, A. P. *Nature* **1991**, *349*, 431−434. (b) Cheng, K. C.; Cahill, D. S.; Kasai, H.; Nishimura, S.; Loeb, L. A. *J. Biol. Chem.* **1992**, *267*, 166−172. (c) Tchou, J.; Grollman, A. P. *Mutat. Res.* **1993**, *299*, 277−287. (d) Kouchakdjian, M.; Bodepudi, V.; Shibutani, S.; Eisenberg, M.; Johnson, F.; Grollman, A. P.; Patel, D. J. *Biochemistry* **1991**, *30*, 1403−1412.

10.1021/jo990059s CCC: $18.00
Published on Web 06/11/1999

electron attachment at lower temperatures, as characterized by ESR spectroscopy:[1b,5−9] cytosine radical anion ($C^{\bullet-}$) and thymine radical anion ($T^{\bullet-}$) are thus produced in 75% and 24% yields, respectively. At higher temperatures, however, an equilibrium involving a mutual electron-transfer process is established between the thymine and cytosine radical anions, from which irreversible protonation at C6 of the thymine radical anion $T^{\bullet-}$ takes place to produce a major intermediate of the 5,6-dihydrothymin-5-yl radical ($TH^{\bullet}$).[10,11] In contrast to oxidative damages, there has been little evidence for the influence of radiation-induced reductive DNA-base damages on biological lesions. Previously, a negative result for the biological effect has been reported that 5,6-dihydrothymine structures incorporated in DNA are responsible for neither a blocking nor a premutagenic lesion,[12] while it is one of the typical damage structures induced by radiolytic reduction of thymine moiety. Although the biological significance of the reductive DNA damages is still obscure, it may be assumed that a reduction mechanism is operative to account for the lethal effect of radiation on hypoxic cells as are involved in solid tumor tissues.[1d]

Previously, we reported efficient formation of C5−C5′-linked dihydrothymidine dimer (**3c**) in the radiolytic one-electron reduction of thymidine (**1c**) in deoxygenated aqueous solution (Scheme 1), in which 5,6-dihydrothymidin-5-yl radicals (**5c**) were assumed as the most likely intermediate species (see also Scheme 2).[13] Possible stereoisomers of the C5−C5′-linked dihydrothymidine dimers have not yet been isolated and characterized, while hydrogenated thymidine stereoisomers as the accompanied major products, (5*S*)-(−)-5,6-dihydrothymidine and (5*R*)-(+)-5,6-dihydrothymidine, were identified[13] by reference to the reported structures.[14] It seems of interest to compare the conformational characteristics of C5−C5′-linked dihydrothymine dimers with those of cyclobutane pyrimidine photodimers possessing not only C5−C5′ but also C6−C6′ linkages, which are afforded through a formal [2 + 2] cycloaddition between the C5−C6 double bonds of adjacent pyrimidines upon UV irradiation of DNA.[1a,15] The pyrimidine photodimers have been identified as highly mutagenic and carcinogenic lesions that result in miscoding during the DNA replication due to perturbations of base-pairing interactions and global structural changes in DNA.[15b] The local and global structures of pyrimidine photodimer-incorporated DNA have been extensively studied by means of computational simulations,[16] NMR spectroscopy,[17] X-ray crystallography,[18] and electrophoresis[19] to get molecular insight into the mechanisms, by which the photodimers induce mutagenicity and in turn interact with a repair enzyme of DNA photolyase.[20] Comparing these structural characterizations with the X-ray crystal structures of DNA-excision repair enzyme and DNA photolyase, it is the most likely that the enzymes may recognize the local structures of the photodimers as well as the whole pattern of small perturbation of the dimer-incorporated DNA.[20]

Scheme 1

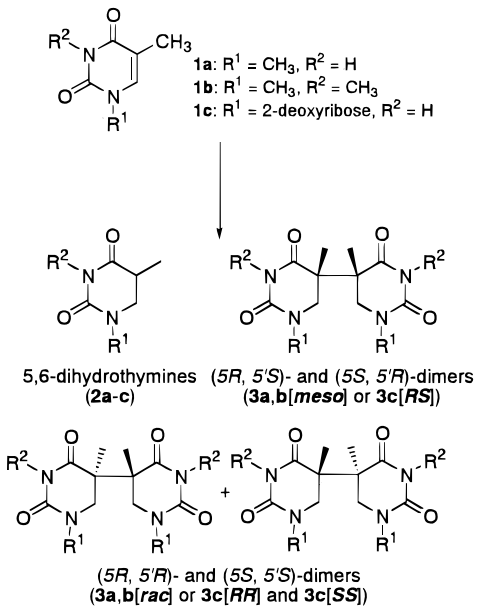

In light of the biological role of pyrimidine photodimers, we have a hypothesis that the C5−C5′-linked dihydrothymine dimers could be potentially mutagenic and carcinogenic lesions when formed by chance at a thymine-thymine (TT) tract in DNA upon exposure of hypoxic cells to ionizing radiation. In this study, radiolytic reductions of N1-substituted thymine derivatives such as 1-methylthymine (**1a**), 1,3-dimethylthymine (**1b**), and thymidine (**1c**) (Scheme 1) in deoxygenated aqueous solution have been performed to isolate stereoisomers of C5−C5′-linked dihydrothymine dimers: the meso form of (5*R*,5′*S*)- and

(5) Symons, M. C. R. In *The Early Effects of Radiation on DNA*; Fielden, E. M., O'Neill, P., Eds.; Springer: Berlin, 1991; Vol. H54, pp 111−124.
(6) Sevilla, M. D. In *Excited States In Organic Chemistry and Biochemistry*; Pullman, B., Goldblum, N., Eds.; D. Reidel: Dordrecht, Holland, 1977.
(7) Sevilla, M. D.; Failor, R.; Clark, C.; Holroyd, R. A.; Pettei, M. *J. Phys. Chem.* **1976**, *80*, 353−358.
(8) Sevilla, M. D.; Becker, D.; Yan, M.; Summerfield, S. R. *J. Phys. Chem.* **1991**, *95*, 3409−3415.
(9) (a) Novais, H. M.; Steenken, S. *J. Am. Chem. Soc.* **1986**, *108*, 1−6. (b) Cullis, P. M.; McClymont, J. D.; Malone, M. E.; Mather, A. N.; Podmore, I. D.; Sweeney, M. C.; Symons, M. C. R. *J. Chem. Soc., Perkin Trans. 2* **1992**, 1695−1702.
(10) (a) Hayon, E. *J. Chem. Phys.* **1969**, *51*, 4881−4899. (b) Theard, L. M.; Peterson, F. C.; Myers, L. S., Jr. *J. Phys. Chem.* **1971**, *75*, 3815−3821. (c) Das, S.; Deeble, D. J.; Schuchmann, M.-N.; von Sonntag, C. *Int. J. Radiat. Biol.* **1984**, *46*, 7−9.
(11) (a) Steenken, S.; Telo, J. P.; Candeias, L. P. *J. Am. Chem. Soc.* **1992**, *114*, 4701−4709. (b) Deeble, D. J.; Das, S.; von Sonntag, C. *J. Phys. Chem.* **1985**, *89*, 5784−5788.
(12) Ide, H.; Petrullo, L. A.; Hatahet, Z.; Wallace, S. S. *J. Biol. Chem.* **1991**, *266*, 1469−1477.
(13) Nishimoto, S.; Ide, H.; Nakamichi, K.; Kagiya, T. *J. Am. Chem. Soc.* **1983**, *105*, 6740−6741.
(14) Cadet, J.; Balland, A.; Berger, M. *Int. J. Radiat. Biol.* **1981**, *39*, 119−133.
(15) (a) Cadet, J.; Vigny, P. In *Bioorganic Photochemistry: Photochemistry and the Nucleic Acids*; Morrison, H., Ed.; John Wiley & Sons: New York, 1990; pp 1−272. (b) Taylor, J.-S. *Acc. Chem. Res.* **1994**, *27*, 76−82.
(16) Miaskiewicz, K.; Miller, J.; Cooney, M.; Osman, R. *J. Am. Chem. Soc.* **1996**, *118*, 9156−9163.
(17) (a) Taylor, J.-S.; Garrett, D. S.; Brockie, I. R.; Svoboda, D. L.; Telser, J. *Biochemistry* **1990**, *29*, 8858−8866. (b) Kan, L.-S.; Voituriez, L.; Cadet, J. *Biochemistry*, **1988**, *27*, 5796−5803. (c) Rycyna, R. E.; Wallace, J. C.; Sharma, M.; Alderfer, J. L. *Biochemistry* **1988**, *27*, 3152−3163.
(18) (a) Camerman, N.; Camerman, A. *Science* **1968**, *160*, 1451−1452. (b) Camerman, N.; Camerman, A. *J. Am. Chem. Soc.* **1970**, *92*, 2523−2527. (c) Hruska, F. E.; Voituriez, L.; Grand, A.; Cadet, J. *Biopolymers* **1986**, *25*, 1399−1417.
(19) (a) Wang, C.-I.; Taylor, J.-S. *Proc. Natl. Acad. Sci. U.S.A.* **1991**, *88*, 9072−9076. (b) Wang, C.-I.; Taylor, J.-S. *Chem. Res. Toxicol.* **1993**, *6*, 519−523.
(20) (a) Park, H.-W.; Kim, S.-T.; Sancar, A.; Deisenhofer, J. *Science* **1995**, *268*, 1866−1872. (b) Vassylyev, D. G.; Kashiwagi, T.; Mikami, Y.; Ariyoshi, M.; Iwai, S.; Ohtsuka, E.; Morikawa, K. *Cell* **1995**, *83*, 773−782.

Scheme 2

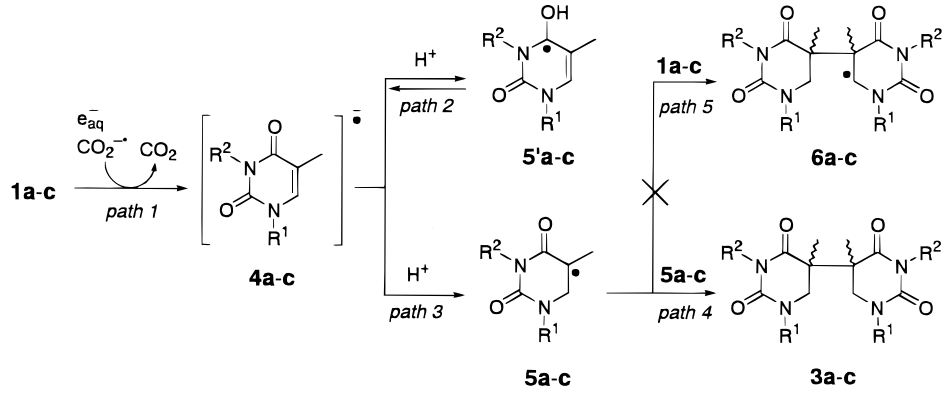

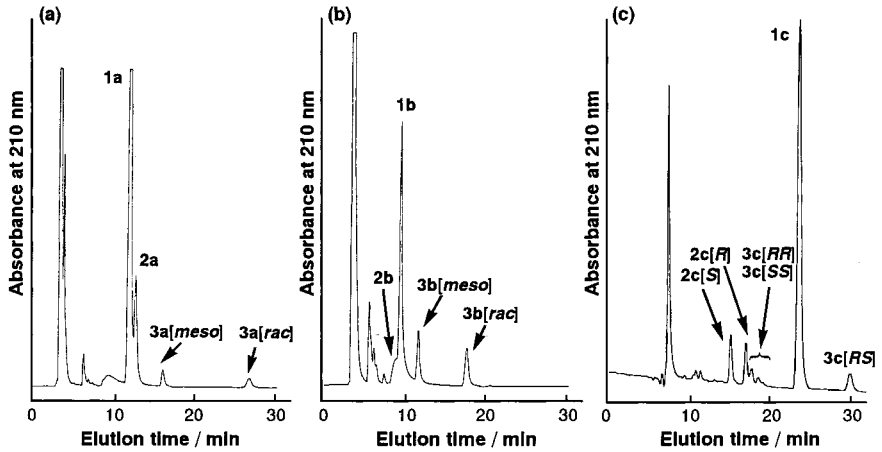

Figure 1. Typical HPLC analyses of phosphate buffer solutions (pH 7.0) of (a) **1a**, (b) **1b**, and (c) **1c** (5 mM) after γ-irradiation (2 kGy) in the presence of sodium formate (200 mM) under Ar, as observed by delivering phosphate buffer solution (pH 3) with (a) 15%, (b) 25%, and (c) 10% of methanol at a flow rate of 0.6 mL min^{-1}. HPLC analysis was performed using (a, b) a Wakosil 5C18 column (ϕ 4.6 mm × 150 mm) or (c) a Cosmosil 5C18 MS column (ϕ 4.6 mm × 250 mm).

(5*S*,5′*R*)-bi-5,6-dihydrothymines (**3a**,**b**[***meso***]) and racemic compounds of (5*R*,5′*R*)- and (5*S*,5′*S*)-bi-5,6-dihydrothymines (**3a**,**b**[***rac***]) from **1a**,**b**, the pseudo-meso form of (5*R*,5′*S*)- and (5*S*,5′*R*)-bi-5,6-dihydrothymidines (**3c**[***RS***]), and two diasterormers of (5*R*,5′*R*)-, and (5*S*,5′*S*)-bi-5,6-dihydrothymidines (**3c**[***RR***] and **3c**[***SS***]) from **1c**. The present structural characterization has provided a prediction that the meso form of the C5−C5′-linked dihydrothymine dimeric structure could be formed at a given TT tract in DNA through a small extent of conformational change.

Results and Discussion

Formation and Characterization of C5−C5′-Linked Dihydrothymine Dimers. For investigating reduction reactivity of 1-methylthymine (**1a**), 1,3-dimethylthymine (**1b**), and thymidine (**1c**) exclusively in the radiolysis of aqueous solution, strongly oxidizing OH radicals generated along with reducing species of hydrated electrons and hydrogen atoms from water radiolysis (see reactions 1 and 3) were effectively scavenged by the aid of well-specified scavengers.[1a] The *G* values[21] of primary water radicals are known as $G(e_{aq}^-) \approx G(^\bullet OH) = 2.8 \times 10^{-7}$ mol J^{-1} and $G(^\bullet H) = 0.6 \times 10^{-7}$ mol J^{-1} in neutral aqueous solution.[1a] In a deoxygenated aqueous solution containing an excess amount of (i) 2-methyl-2-propanol ($(CH_3)_3COH$) or (ii) formate ions ($HCOO^-$), OH radicals and hydrogen atoms are scavenged into substantially unreactive 2-methyl-2-propanol radicals (reaction 4: $k(^\bullet OH) = 5 \times 10^8$ dm^3 mol^{-1} s^{-1} as a major reaction, $k(^\bullet H) = 8 \times 10^4$ dm^3 mol^{-1} s^{-1} as a minor reaction) or converted to a somewhat less reducing species of carbon dioxide radical anions ($CO_2^{\bullet -}$; $G(CO_2^{\bullet -}) = 3.5 \times 10^{-7}$ mol J^{-1}) (reaction 5: $k(^\bullet OH) = 3 \times 10^9$ dm^3 mol^{-1} s^{-1}, $k(^\bullet H) = 3 \times 10^8$ dm^3 mol^{-1} s^{-1}), respectively.[1a] Consequently, the reaction systems involving the restricted radical species for exclusive reduction can be achieved: (i) e_{aq}^- (reduction potential at pH 7.0: $E(nH_2O/e_{aq}^-) = -2.9$ V vs NHE[22]) + $^\bullet H$ ($E(H^+/^\bullet H) = -2.4$ V[22]) and (ii) $e_{aq}^- + CO_2^{\bullet -}$ ($E(CO_2/CO_2^{\bullet -}) = -1.9$ V[23]).

$$(CH_3)_3COH + {}^\bullet OH\ ({}^\bullet H) \rightarrow {}^\bullet CH_2(CH_3)_2COH + H_2O\ (H_2) \quad (4)$$

$$HCOO^- + {}^\bullet OH\ ({}^\bullet H) \rightarrow CO_2^{\bullet -} + H_2O\ (H_2) \quad (5)$$

Figure 1a−c shows representative HPLC chromatograms as monitored by UV absorbance at 210 nm for Ar-purged phosphate buffer solutions (5 mM, pH 7.0) of N1-substituted thymine derivatives **1a**−**c**, respectively, after

(21) The number of molecules produced or changed per 1 J of radiation energy absorbed by the reaction system.

(22) Swallow, A. J. In *Radiation Chemistry. An Introduction*; Longman: London, 1973.

(23) Schwarz, H. A.; Creutz, C.; Sutin, N. *Inorg. Chem.* **1985**, *24*, 433−439.

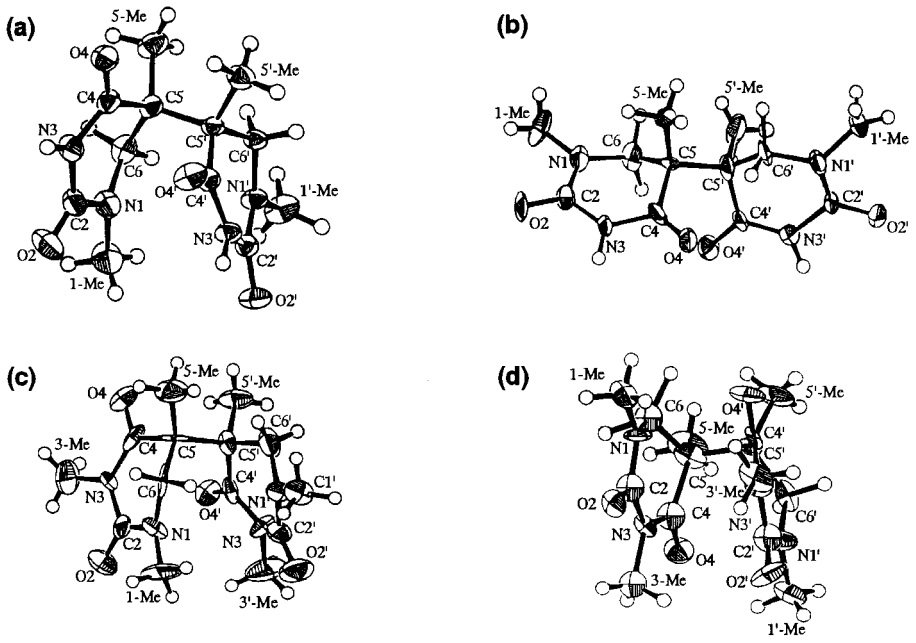

Figure 2. ORTEP drawings of C5−C5′-linked dihydrothymine dimers: (a) **3a**[***meso***]; (b) **3a**[***rac***]; (c) **3b**[***meso***]; (d) **3b**[***rac***].

2 kGy γ-irradiation in the presence of excess (1 M) sodium formate. Most of the products could not be detected by UV absorption at 254 nm, indicating the efficient formation of C5−C6-saturated thymine structures in the reduction of **1a**−**c** with hydrated electrons and $CO_2^{\bullet-}$ as well. The eluents from the respective major peaks were collected by preparative HPLC and fractionation. The fractionated products in aqueous solution containing 10−25 vol % methanol were evaporated at room temperature and submitted to a purity check by analytical HPLC followed by spectroscopic characterization. High-resolution positive FAB mass spectrometry (FAB−HRMS) of the isolated HPLC fractions **2a**−**c** (single peak for **2a**,**b** in Figure 1a,b and double peaks for **2c** in Figure 1c) and **3a**−**c** (double peaks for **3a**,**b** in Figure 1a,b and triple peaks for **3c** in Figure 1c) provided protonated parent ions that are in accord with the molecular formulas of the corresponding 5,6-dihydrothymine derivatives and C5−C5′-linked dihydrothymine dimers, respectively (see the Experimental Section). According to the ^{1}H and ^{13}C NMR spectral data by reference to authentic samples, the products **2a**,**b** were identified as 1-methyl-5,6-dihydrothymine (**2a**) and 1,3-dimethyl-5,6-dihydrothymine (**2b**), respectively. Similar products derived from hydrogenation of **1c** were stereoisomeric and identified as 5(*S*)-(−)-5,6-dihydrothymidine (**2c**[***S***]) and 5(*R*)-(+)-5,6-dihydrothymidine (**2c**[***R***]) by comparing the spectral data with those of authentic samples.[13,14] These 5,6-dihydrothymine derivatives are well documented products obtained in the radiolytic reduction of thymine derivatives in aqueous solution. In separate experiments, the HPLC fractions eluted in shorter retention times (<5 min) in Figure 1a−c were confirmed to contain relatively low yields of C5- and/or C6-carboxylated byproducts resulting from addition of $CO_2^{\bullet-}$ to the C5−C6 double bond of **1a**−**c**.[24,25] As expected, such a carboxylation was excluded in the radiolysis of aqueous solution containing excess 2-methyl-2-propanol instead of sodium formate.

Since the FAB−HRMS data predict that the products **3a**−**c** may be isomeric C5−C5′-linked dihydrothymine dimers, attempts were made to determine their crystal structures by X-ray crystallography. By reference to the crystallographs of **3a**,**b** in Figure 2 (see also Chart 1), we determined that the faster HPLC fractions are the meso forms of the (5*R*,5′*S*)-bi-5,6-dihydrothymine derivatives (**3a**,**b**[***meso***]), while the slower HPLC fractions are racemic compounds of (5*R*,5′*R*)- and (5*S*,5′*S*)-bi-5,6-dihydrothymine derivatives (**3a**,**b**[***rac***]) (see also Figure 1a,b). In the present study, further separation of the racemic compounds **3a**,**b**[***rac***] was not performed. In contrast to **3a**,**b**, the crystals of the three HPLC fractions of **3c** were unstable, and therefore, their X-ray crystallographic data were collected by coating with 40 vol % collodion−ethanol solution to identify only **3c**[***RS***]: the X-ray crystallography in collodion-coating and in a capillary tube was unsuccessful for the other two products. Figure 3 illustrates the structure and the three-dimensional lattice packing diagram of **3c**[***RS***], indicating that a pair of (5*S*,5′*R*)-bi-5,6-dihydrothymidine and (5*R*,5′*S*)-bi-5,6-dihydrothymidine monohydrates are packed in a unit cell: there is a hydrogen bond between the crystal water and one of the deoxyribose-C(5)−OH groups of the dimer. Although crystal structures are unknown, the

Chart 1

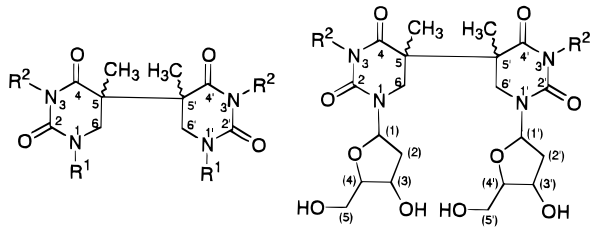

(24) Various carboxylated monomeric and dimeric thymine derivatives were separated by HPLC when phosphate buffer solutions (10 mM, pH 3.0) contained higher contents of methanol (10−25 vol %). The structural characterization by X-ray crystallography of 5,6-dihydrothymine-6-carboxylic acid as a major product among them was performed to get insight into the inhibitory effect on dihydroorotate dehydrogenage and will be reported elsewhere (Ito, T.; Hatta, H.; Nishimoto, S. Manuscript in preparation).

(25) Wada, T.; Ide, H.; Nishimoto, S.; Kagiya, T. *Int. J. Radiat. Biol.* **1982**, *42*, 215−221.

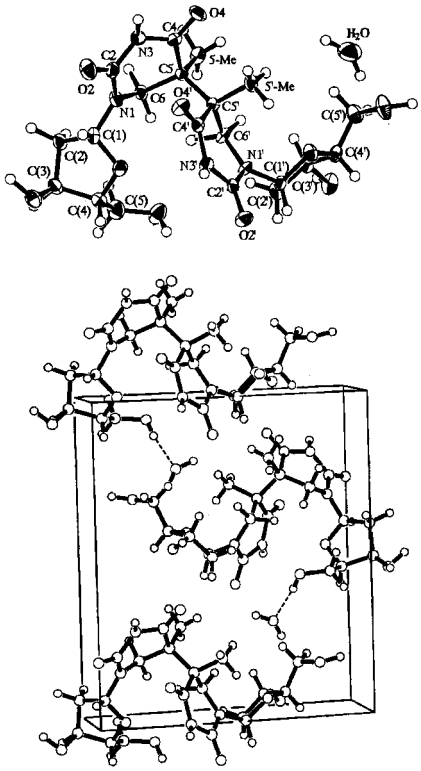

Figure 3. ORTEP drawing and a three-dimensional lattice packing diagram of C5−C5′-linked dihydrothymidine dimer (**3c**[***RS***]).

accompanying two products may be assigned to diastereoisomeric (5*R*,5′*R*)-bi-5,6-dihydrothymidine (**3c**[***RR***]) and (5*S*,5′*S*)-bi-5,6-dihydrothymidine (**3c**[***SS***]), respectively, in accord with the ^{1}H and ^{13}C NMR data (Tables 5 and 6). As implicated from Figure 3, the C5−C5′-linked dihydrothymidine dimer bearing hydrophilic deoxyribose moiety favor the crystallization in the form of hydrate, while dehydration of the resulting crystal would cause readily a lattice decomposition. In this context, it is noteworthy that the pseudo-meso form **3c**[***RS***] is eluted slower than the diastereomers **3c**[***RR***] and **3c**[***SS***] in the HPLC, opposite to the elution speeds of **3a**,**b**[***meso***] being faster than those of **3a**,**b**[***rac***] (Figure 1a−c). It is likely that the hydrocarbon component of the 2-deoxyribose moiety is involved in hydrophobic interactions, and therefore, the accessibility of the furanose ring may play some role in the HPLC behavior of C5−C5′-linked dihydrothymidine dimers.

The X-ray crystallographic data are summarized in Tables 1 and 2. The C5−C5′-linked dihydrothymine dimers **3a**−**c** possess the C5−C5′ bond lengths from 1.55 to 1.59 Å. These are comparable to both the C5−C5′ and C6−C6′ bond lengths of photodimers: 1.58 and 1.60 Å for the *cis-syn*-1,3-dimethylthymine cyclobutane photodimer[18b] and 1.548 and 1.596 Å for 1,1′-trimethylenebisthymine photodimer (Thy-[C$_3$]-Thy(*c*,*s*)).[26] According to the crystal structures shown in Figures 2 and 3, two pyrimidine rings of the C5−C5′-linked dihydrothymine dimers **3a**−**c** overlap with each other, the extent of which was evaluated by the dihedral angles between the pyrimidine-containing planes composed of N1, N3, and C5 atoms. The calculation indicates 128° for **3a**[***meso***], 160° for **3a**[***rac***], 134° for **3b**[***meso***], 136° for **3b**[***rac***], and 113° for **3c**[***RS***]. Except for the result for **3a**[***rac***], these dihedral angles are considerably smaller than the corresponding values of 152° (N1−N3−C5 planes) and 153° (C2−C4−C6 planes) for the *cis-syn*-1,3-dimethylthymine cyclobutane photodimer and 178° for Thy-[C$_3$]-Thy(*c*,*s*). It was also demonstrated that the pyrimidine rings of **3a**−**c** are not planar where the C6 atoms are out of the planes of the other atoms. Furthermore, the pyrimidine rings of **3a**−**c** are twisted around the C5−C5′ linkage, and the torsion angles through 5-Me-C5−C5′-5′-Me vary significantly in the range of 43−85°. These values are much greater than 24° for the *cis-syn*-1,3-dimethylthymine photodimer because the absence of the C6−C6′ linkage in **3a**−**c** permits more free rotation of pyrimidine rings around the C5−C5′ linkage. Nevertheless, it is interesting that two pyrimidine rings of **3a**,**b**[***meso***] are confronted with each other and thereby cause a stacking of their carbonyl groups as in the *cis-syn*-cyclobutane photodimers. By reference to the twist angle for a successive thymine base pair about the axis of DNA duplex, e.g., 33−39° for the structure of GCGTTTTTTCGC,[27] it seems structurally feasible that the meso form of a C5−C5′-linked dihydrothymine dimer structure like **3a**[***meso***] could be produced at a successive thymine base pair by reduction pathway to cause some distortion within a DNA duplex. Similar to *cis-syn* photodimers, such a meso dimer structure may give rise to insufficient stacking of the pyrimidine rings that will weaken the hydrogen bonds of the 3′- or 5′-dihydrothymine moiety with complementary adenine. In contrast to the meso dimer, the formation of racemic compounds of C5−C5′-linked dihydrothymine dimers such as **3a**[***rac***] from the normal stacking conformation of adjacent thymines in DNA is unlikely, since two pyrimidine rings should be arranged in the almost identical plane without overlapping of their carbonyl groups.

The ^{1}H and ^{13}C NMR data in D$_2$O or dimethyl sulfoxide-d_6 are consistent with the crystallographic characterizations of C5−C5′-linked dihydrothymine dimers **3a**−**c** (Tables 3−6). Table 3 compares the ^{1}H NMR data between **3a**,**b**[***meso***] and **3a**,**b**[***rac***] for better understanding of the conformations in solution. For each dimer, the meso form and the racemic form had similar ^{1}H NMR chemical shifts except for the H6 and H6′ resonance. It is thus remarkable that **3a**,**b**[***meso***] showed downfield shifts in the H6 resonance and in turn upfield shifts in the counterpart H6′ resonance; therefore, the H6 and H6′ chemical shifts become closer to each other relative to **3a**,**b**[***rac***]. Similarly, the H6 and H6′ chemical shifts of **3c**[***RS***] were also closer to each other, compared with those of **3c**[***RR***] or **3c**[***SS***], although both protons showed relatively upfield shifts (Table 5). On the other hand, the ^{13}C NMR chemical shifts showed little difference between the isomers (Tables 4 and 6).

Mechanism of C5−C5′-Linked Dimerization by Radiolytic Reduction. Previously, we reported a brief account for the mechanism by which thymidine undergoes one-electron reduction by hydrated electron or $CO_2^{\bullet-}$ to give C5−C5′-linked dihydrothymidine dimer and 5,6-dihydrothymidines.[13] Thymine is known to undergo one-electron reduction into its radical anion by hydrated electron at a diffusion-controlled rate ($k(e_{aq}^-) = 1.7 \times 10^{10}$ dm^3 mol^{-1} s^{-1} at pH 6.0)[28] and similarly by $CO_2^{\bullet-}$ at more

(26) Leonard, N. J.; Golankiewicz, K.; McCredie, R. S.; Johnson, S. M.; Paul, I. C. *J. Am. Chem. Soc.* **1969**, *91*, 5855−5862.
(27) Nelson, H. C. M.; Finch, J. T.; Luisi, B. F.; Klug, A. *Nature* **1987**, *330*, 221−226.

Table 1. Crystal Data and Experimental Details

	3a[*meso*]	**3a**[*rac*]	**3b**[*meso*]	**3b**[*rac*]	**3c**[*RS*]
a (Å)	8.618(5)	20.645(6)	8.375(4)	13.24(1)	6.000(3)
b (Å)	11.898(4)	6.414(4)	10.602(6)	15.50(1)	14.619(2)
c (Å)	13.020(5)	12.186(4)	17.480(3)	14.73(1)	13.280(2)
β (°)	97.23(5)	121.29(2)	100.79(2)		102.12(2)
V (Å^3)	1324(1)	1378.9(9)	1524(1)	3022(3)	1138.8(6)
Z	4	4	4	8	2
μ (Mo Kα) (cm^{-1})	1.08	1.04	1.00	1.01	1.20
space grp	$P2_1/c$	Cc	$P2_1/n$	$Pbcn$	$P2_1$
cryst syst	monoclinic	monoclinic	monoclinic	orthorhombic	monoclinic
residuals[a] (*R*; R_w)	4.3; 4.9	5.5; 6.6	7.7; 4.9	6.0; 3.7	4.8; 6.0
GOF	1.55	2.17	2.64	1.74	2.58

[a] $R = \Sigma||F_o| - |F_c||/\Sigma|F_o|$; $R_w = [(\Sigma w(|F_o| - |F_c|)^2/\Sigma w|F_o|^2)]^{1/2}$.

Table 2. Selected Bond Length, Plain Angles, and Torsion Angles ofC5−C5′-Linked Dihydrothymine Dimers

	3a[*meso*]	**3a**[*rac*]	**3b**[*meso*]	**3b**[*rac*]	**3c**[*RS*]
bond length (Å)					
C5−C5′	1.591(3)	1.568(4)	1.57(2)	1.55(2)	1.583(6)
N1−C2	1.347(3)	1.39(1)	1.36(2)	1.35(2)	1.348(5)
C2−N3	1.364(3)	1.34(1)	1.41(2)	1.41(2)	1.393(6)
N3−C4	1.395(3)	1.410(8)	1.37(2)	1.35(2)	1.379(5)
C4−C5	1.530(3)	1.541(10)	1.56(2)	1.60(2)	1.534(6)
C5−C6	1.530(3)	1.55(1)	1.50(2)	1.53(2)	1.544(5)
C6−N1	1.457(3)	1.455(9)	1.49(2)	1.48(2)	1.459(5)
N1′−C2′	1.339(2)	1.27(1)	1.35(2)	1.35(2)	1.354(5)
C2′−N3′	1.385(2)	1.47(1)	1.40(2)	1.44(2)	1.385(5)
N3′−C4′	1.366(2)	1.348(9)	1.36(2)	1.38(2)	1.372(6)
C4′−C5′	1.528(3)	1.50(1)	1.57(2)	1.56(2)	1.524(6)
C5′−C6′	1.537(3)	1.54(1)	1.51(2)	1.55(2)	1.542(6)
C6′−N1′	1.463(2)	1.457(9)	1.46(2)	1.44(2)	1.467(5)
plane angle (deg) between pyrimidine rings					
	128	160	134	136	113
torsion angle (deg) about C5−C5′					
	51.1(2)	−85.4(4)	−65(1)	43(2)	64.9(4)

Table 3. ^{1}H NMR (DMSO-d_6, 270 MHz) Chemical Shifts (ppm) of C5−C5′-Linked Dihydrothymine Dimers

	3a[*meso*]	**3a**[*rac*]	**3b**[*meso*]	**3b**[*rac*]
5-CH_3	1.184 (s)	1.136 (s)	1.167 (s)	1.084 (s)
1-CH_3	2.794 (s)	2.875 (s)	2.804 (s)	2.814 (s)
3-CH_3			2.908 (s)	2.892 (s)
3-NH	10.143 (s)	10.100 (s)		
H_{6A}, $H_{6'A}$	3.208 (d)	3.003 (d)	3.263 (d)	3.127 (d)
H_{6B}, $H_{6'B}$	3.440 (d)	4.143 (d)	3.383 (d)	3.734 (d)
J_{AB} (Hz)	−13.5	−12.2	−13.8	−12.7

Table 4. ^{13}C NMR (DMSO-d_6, 67.5 MHz) Chemical Shifts (ppm) of C5−C5′-Linked Dihydrothymine Dimers

	3a[*meso*]	**3a**[*rac*]	**3b**[*meso*]	**3b**[*rac*]
5-CH_3	18.781	15.957	19.225	17.338
1-CH_3	33.743	34.366	34.818	35.590
3-CH_3			27.814	27.843
C_5	44.982	43.822	45.572	44.689
C_6	51.932	52.482	50.509	50.442
C_2	152.870	151.972	153.471	152.389
C_4	173.223	175.295	172.435	173.368

than 5 orders of magnitude slower rate ($k(CO_2^{\bullet-}) = \sim 5 \times 10^4$ dm^3 mol^{-1} s^{-1}).[28] By reference to the reduction potential[23] vs the normal hydrogen electrode at pH 7.0, $CO_2^{\bullet-}$ ($E(CO_2/CO_2^{\bullet-}) = -1.9$ V) is of less reducing ability than hydrated electron ($E(nH_2O/e_{aq}^-) = -2.9$ V). Nevertheless, we confirmed in the previous study[13] that $CO_2^{\bullet-}$ had practically the same one-electron reducing ability as hydrated electron toward **1c**, thus resulting in similar product distribution of **2c**[***R***], **2c**[***S***], and **3c** (the stereoisomers were not separated previously).

(28) Buxton, G. V.; Greenstock, C. L.; Helman, W. P.; Ross, A. B. *J. Phys. Chem. Ref. Data* **1988**, *17*, 513−886.

Table 5. ^{1}H NMR (D_2O, 400 MHz) Chemical Shifts (ppm) of C5−C5′-Linked Dihydrothymidine Dimers

	3c[*RS*]	**3c**[*RR*] or **3c**[*SS*]
5-CH_3	1.278 (s), 1.305 (s)	1.139 (s), 1.222 (s)
H_{6A}, $H_{6'A}$	3.275 (d), 3.323 (d)	3.335 (d), 3.176 (d)
H_{6B}, $H_{6'B}$	3.578−3.680[a] (m)	4.061 (d), 4.090 (d
J_{6AB}, $J_{6'AB}$ (Hz)	−13.6, −13.2	−12.2, −13.0
deoxyribose		
$H_{(1)}$	6.127 (t), 6.077 (t)	6.174 (t), 6.233 (t)
$H_{(2)}$	1.982−2.189 (m)	1.985−2.221 (m), 2.059−2.252 (m)
$H_{(3)}$	4.232−4.280 (m)	4.247−4.282 (m), 4.285−4.310 (m)
$H_{(4)}$	3.764−3.794 (m)	3.778−3.806 (m), 3.797−3.826 (m)
$H_{(5)}$	3.548−3.645[a] (m)	3.568−3.666 (m), 3.552−3.667 (m)

[a] A part of the H_6 peaks overlapped with the $H_{(5)}$ peaks.

Table 6. ^{13}C NMR (D_2O, 100 MHz) Chemical Shifts (ppm) of C5−C5′-Linked Dihydrothymidine Dimers

	3c[*RS*]	**3c**[*RR*] or **3c**[*SS*]
5-CH_3	20.394, 20.504	17.505, 17.359
C_6	46.235, 46.528	47.333, 47.278
C_2	156.366, 156.622	155.525, 156.257
C_4	178.220, 178.330	179.828, 179.812
C_5	47.497, 47.698	46.894, 47.845
deoxyribose		
$C_{(1)}$	86.798, 86.835	86.652, 86.908
$C_{(2)}$	37.860, 38.116	38.006, 38.281
$C_{(3)}$	73.594, 73.631	73.503, 73.448
$C_{(4)}$	87.987, 88.060	88.060, 88.006
$C_{(5)}$	64.139, 64.286	63.993, 64.048

For the clarity of the mechanism of C5−C5′-linked dimerization, a further attempt was made to investigate the influence of pH on the radiolytic reduction of **1a**−**c** in anoxic buffer solution. As shown in Figure 4, upon increasing the pH values from 3.0 to 11.0, the *G* values for both the decomposition of **1a**,**b** and the formation of C5−C5′-linked dimers **3a**,**b** increased in acidic solution, attained their maxima in neutral solution, and then decreased in basic solution. Similar behavior was also observed for the radiolytic reduction of **1c** into **3c**, while the pH value resulting in the maximum *G* values shifted to somewhat basic region of pH 9.0. In a wide pH range the stereoisomeric C5−C5′-linked dimers as the meso form and the racemic compounds were produced in almost equivalent yields. The maximum *G* values of the respective C5−C5′-linked dimers thus obtained were **3a**[***meso***] = 1.07×10^{-7} mol J^{-1} (23% selectivity based on the decomposed substrate), **3a**[***rac***] = 0.97×10^{-7} mol J^{-1} (20%), **3b**[***meso***] = 1.02×10^{-7} mol J^{-1} (30%), and **3b**[***rac***] = 0.91×10^{-7} mol J^{-1} (27%) for **3c**[***RS***] = 1.22×10^{-7} mol J^{-1} (20%) and for **3c**[***RR***] + **3c**[***SS***] = 1.13×10^{-7} mol J^{-1} (18%).

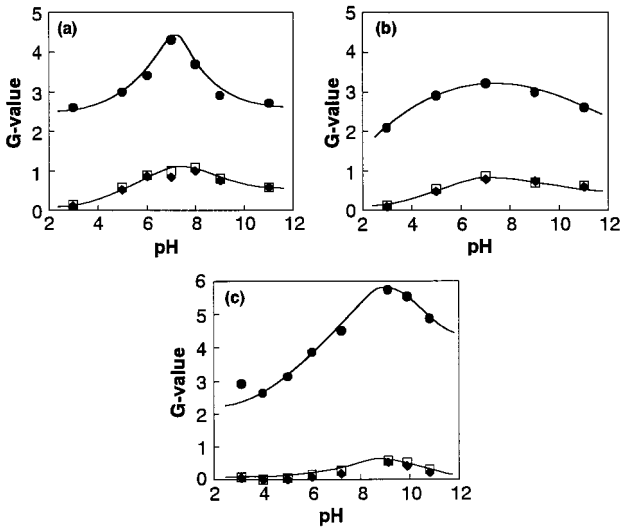

Figure 4. pH-dependent variation of *G* values for decomposition of thymine derivatives (●, **1a**−**c**) and formation of C5−C5′-linked dihydrothymine dimers (◆, **3a**,**b**[***meso***] or **3c**[***RS***]; □ **3a**,**b**[***rac***] or **3c**[***RR***] + **3c**[***SS***]) in the γ-radiolysis of Ar-purged phosphate buffer solution containing sodium formate (200 mM): C5−C5′-linked dimerization of (a) **1a** to **3a**, (b) **1b** to **3b,** and (c) **1c** to **3c**.

In light of previous studies on the reaction of hydrated electrons with pyrimidines,[10] the pH dependence of the C5−C5′-linked dimerization may be rationalized by the reaction pathways given in Scheme 2. The initial and key step involves one-electron reduction of **1a**−**c** by not only hydrated electron but also by $CO_2^{\bullet-}$ to form the corresponding radical anions as the primary intermediates (**4a**−**c**) (path 1). It is likely that the electron adducts **4a**−**c** are readily protonated at O4 by water (path 2) to form the reducing radicals (**5′a**−**c**) followed by very slow self-termination.[1a] In view of the p$K_a \approx 7.2$ for the protonated electron adduct of thymine,[10] such protonations of **4a**−**c** will become more significant with decreasing the pH, and inversely, deprotonation of **5′a**−**c** (path 2) will be more facilitated with increasing pH value. In competition with the fast protonation at O4 to oxygen-protonated radicals, **4a**−**c** may also undergo another type of protonation at C6 to form 5,6-dihydrothymin-5-yl radicals (**5a**−**c**) (path 3) that have oxidizing properties and more stability.[29] This reaction occurs irreversibly to increasing extents as the pH decreases; therefore, both the one-electron reductive decomposition and the C5−C5′-linked dimerization by a radical coupling mechanism of **1a**−**c** (path 4) are enhanced. In basic solution at pH > 10, however, the yields of electron adducts **4a**−**c** should significantly decrease in correspondence with the pH effect on the yield of primary active species in the water radiolysis: the yield of OH radicals responsible for the formation of $CO_2^{\bullet-}$ in reaction 5 rapidly decreases, while that of hydrated electrons slightly increases, with increasing pH.[30] There is an additional pH effect on the acidic reaction system in the presence of excess formate ions. In accord with the p$K_a = 3.75$ for formic acid, the formate ions involved in the reaction system for conversion of OH radicals to reducing $CO_2^{\bullet-}$ (see reaction 5) are largely protonated in acidic solution at pH <3.75. Hydrogen abstraction by OH radical from formic acid as in reaction 6 produces a radical species of •COOH that has a stronger acidity (p$K_a = 1.4$) than the parent formic acid and is dissociative into $CO_2^{\bullet-}$ under the present conditions at pH >2.0. However, the rate constant of reaction 5 (k(•OH) $= 3 \times 10^9$ dm^3 mol^{-1} s^{-1}) is 1 order of magnitude greater than that (k(•OH) $= 1 \times 10^8$ dm^3 mol^{-1} s^{-1}) of reaction 6;[28] therefore, the net efficiency of scavenging OH radicals to reducing $CO_2^{-\bullet}$ being lowered to considerable extent in acidic solution at pH < 3.75.

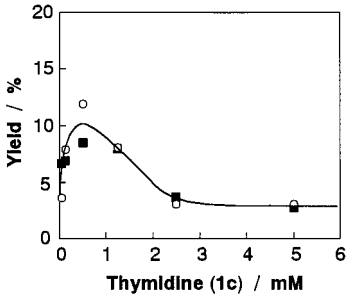

Figure 5. Influence of the concentration of thymidine (**1c**) on the yields of C5−C5′-linked dihydrothymidine dimers (○, **3c**[***RS***]; ■, **3c**[***RR***] + **3c**[***SS***]) as observed at about 30% decomposition of **1c** in the X-radiolysis of Ar-purged phosphate buffer solution (pH 7.0) containing sodium formate (200 mM).

$$HCOOH + {}^{\bullet}OH\ ({}^{\bullet}H) \rightarrow {}^{\bullet}COOH + H_2O\ (H_2) \quad (6)$$

Hydrogen atoms and OH radicals readily add to the C5−C6 double bond of pyrimidines to produce both 5-yl and 6-yl radicals.[1a] We therefore examined a hypothetical radical reactivity whether the C5 radical can add to the C5−C6 double bond of the parent thymine moiety, producing the C5−C5′-linked dimer 6-yl radical (path 5 in Scheme 2), in the representative radiolytic reduction of **1c** in phosphate buffer. As shown in Figure 5, while the yields of **3c** were almost constant at concentrations of **1c** lower than 0.5 mM in formate-containing phosphate buffer (pH 7.0), they were decreased with increasing concentration of **1c**. This result may rule out the above hypothesis that the addition reaction of the 5-yl radical **5c** to the C5 position of the C5−C6 double bond of **1c** will be a notable route to dimeric product **3c**, because it should favor the higher concentrations of **1c** contrary to the results in Figure 5. Figure 5 suggests that contribution of possible hydrogen abstraction of **5c** from the deoxyribose moiety of **1c** may become more important and thereby inhibit the radical coupling to **3c**, upon increasing the concentration of **1c**. In the separate experiments using methanol-d_4 as an OH radical scavenger, radiolytic reduction of **1a**,**b** in phosphate buffer also afforded the C5−C5′-linked dimers **3a**,**b**. Assuming a radical addition mechanism by which the dihydrothymine dimer 6-yl radicals (**6a**,**b**) will be produced from the reaction of C5 radicals **5a**,**b** with **1a**,**b** and thereafter abstract deuterium atom from CD_3OD (Scheme 3), the dimeric products **3a**,**b** should possess the monodeuterated structures. The FAB-MS data of **1a** and **1b** provided the respective parent ions at 283 and 311, demonstrating that the incorporation of deuterium atom into the dimer did not occur. This result is also consistent with the conclusion that the radical coupling mechanism is predominant for the C5−C5′-linked dimerization by radiolytic reduction (path 4).

(29) Whillans, D. W.; Johns, H. E. *J. Phys. Chem.* **1972**, *76*, 489−493.
(30) Spinks, J. W.; Woods, R. J. In *Introduction to Radiation Chemistry*, 3rd ed.; John Wiley & Sons: New York, 1990.

Scheme 3

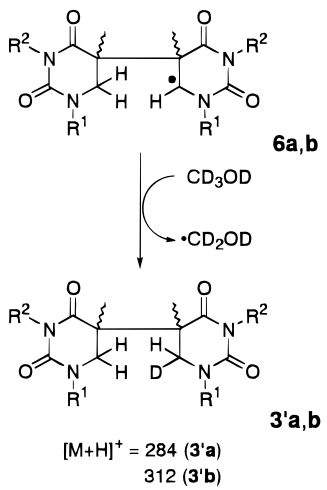

From the redox properties of the oxygen-protonated and carbon-protonated pyrimidine radicals,[10c] it may be expected that disproportionation of radicals by electron transfer from reducing radicals **5′a**−**c** to oxidizing 5-yl radicals **5a**−**c** (path 6) may occur especially in acidic and neutral solutions to reproduce 5,6-dihydrothymines **2a**−**c** along with regeneration of **1a**−**c**, as shown in Scheme 4. However, this disproportionation would not be an important route to **2a**−**c** because the 5-yl radical does not readily undergo electron-transfer reactions,[29] thus being rather of neutral radical nature than oxidizing. Such a neutral radical nature of **5a**−**c** accounts for ready bimolecular radical coupling to form C5−C5′-linked dihydrothymine dimers **3a**−**c** as the major products.

It is likely that the 5-yl radicals are a common intermediate for competition between radical coupling into C5−C5′-linked dimer and hydrogen abstraction into 5,6-dihydrothymine. This competition kinetics was confirmed in the radiolytic reduction of **1c** (0.1 mM) in Ar-saturated phosphate buffer (pH 7.0) with various concentrations of formate ions as a hydrogen donor. As shown in Figure 6, the yields of 5,6-dihydrothymidines **2c**[***S***] and **2c**[***R***] increased, and inversely, those of the C5−C5′-linked dimers **3c** decreased upon increasing the concentration of sodium formate. Another support was that the yields of **2a**,**b** were 2-fold depressed, i.e., about 60% yield with formate to 30% yield with 2-methyl-2-propanol, when the radiolytic reduction of **1a**,**b** was performed in Ar-purged phosphate buffer (pH 7.0) containing 2-methyl-2-propanol (100 mM) instead of sodium formate.

Biological Implication of C5−C5′-Linked Dihydrothymine Dimers. Radiation biological studies have shown that direct ionization of DNA generates DNA radical cations (holes) and electrons to result in fixation of DNA damages.[1] There have also been several results indicating that DNA is able to transport hole[31] and electron[32−35] through a DNA π-stack.[3] In association with the intra-DNA electron migration, previous ESR studies evaluated the relative abundance of DNA-base radical anions (electron−base adducts) as about 75% for the cytosine site and 25% for the thymine site, respectively.[8] The electron adduct of the thymine site seems to be protonated at the C6 to form the 5-yl radical, in accord with the formation of the 5,6-dihydrothymine structure as a major damage fragment in the γ-irradiated aqueous solution of *E. coli* DNA.[36] In the model reactions, the C6-protonation of the electron−thymine adduct occurs more slowly than the corresponding O4-protonation ($k < 2 \times 10^4$ s^{-1})[37] and the N3 protonation ($k = 3.3 \times 10^6$ s^{-1})[38] of the electron−cytosine adduct. Recently, it has also been suggested that the 5,6-dihydrothymin-5-yl radical generated within the DNA duplex may be a precursor to alkaline-labile 2′-deoxyribonolactone generated via radical abstraction of a hydrogen atom at C1′ of the adjacent deoxyribose unit.[39]

According to the present mechanistic study in a model reaction system, it may be postulated that the C5−C5′-linked dihydrothymine dimer structure could be produced by coupling of a pair of thymin-5-yl radicals when generated thorough migration of two electrons to a given adjacent thymine-thymine sequence of DNA. Such a hypothetical C5−C5′-linked dimerization in DNA may not occur by sparsely ionizing low LET radiations under usual conditions due to a mechanistic restriction, even though it seems to be structurally feasible. However, the densely ionizing high LET radiations may permit generation of two electrons as the net for migration and reduction to form an adjacent electron−thymine adduct pair. Recently, the effect of high LET O^{7+} heavy ion beam on thymidine in the solid state has been investigated to identify several dimeric structures among the thymidine decomposition products.[40] These dimeric products are possibly attributed to coupling of several types of monomeric radicals that should be more enhanced by densely ionizing high LET radiations to generate nonhomogeneously high concentration of radicals, relative to sparsely ionizing low LET radiations.

Experimental Section

Materials. 1-Methylthymine (Sigma Chemical), thymine (Kohjin), and thymidine (Kohjin) were used as received. Purified 1,3-dimethylthymine was kindly supplied by Fujii Memorial Research Institute, Otsuka Pharmaceutical. Sodium formate and 2-methyl-2-propanol were purchased from Nacalai Tesque and were used without further purification. NaH_2PO_4 and methanol (HPLC grade) were used as received from Wako Pure Chemical Industries.

(31) (a) Saito, I.; Takayama, M.; Sugiyama, H.; Nakatani, K.; Tsuchida, A.; Yamamoto, M. *J. Am. Chem. Soc.* **1995**, *117*, 6406−6407. (b) Sugiyama, H.; Saito, I. *J. Am. Chem. Soc.* **1996**, *118*, 7063−7068. (c) Breslin, D. T.; Schuster, G. B. *J. Am. Chem. Soc.* **1996**, *118*, 2311−2319.

(32) Dandliker, P. J.; Holmlin, R. E.; Barton, J. K. *Science* **1997**, *275*, 1465−1468.

(33) (a) Murphy, C. J.; Arkin, M. R.; Jenkins, Y.; Ghatlia, N. D.; Bossmann, S. H.; Turro, N. J.; Barton, J. K. *Science* **1993**, *262*, 1025−1029. (b) Arkin, M. R.; Stemp, E. D. A.; Holmlin, R. E.; Barton, J. K.; Hörmann, A.; Olson, E. J. C, Barbara, P. F. *Science* **1996**, *273*, 475−480. (c) Holmlin, R. E.; Dandliker, P. J.; Barton, J. K. *Angew. Chem., Int. Ed. Engl.* **1997**, *36*, 2714−2730. (d) Olson, E. J. C.; Hu, D.; Hörmann, A.; Barbara, P. F. *J. Phys. Chem. B* **1997**, *101*, 299−303.

(34) Murphy, C. J.; Arkin, M. R.; Ghatlia, N. D.; Bossmann, S.; Turro, N. J.; Barton, J. K. *Proc. Natl. Acad. Sci. U.S.A.* **1994**, *91*, 5315−5319.

(35) Netzel, T. L. *J. Chem. Educ.* **1997**, *74*, 646−651.

(36) Téoule, R.; Bonicel, A.; Bert, C.; Fouque, B. *J. Am. Chem. Soc.* **1978**, *100*, 6749−6750.

(37) Shragge, P. C.; Hunt, J. W. *Radiat. Res.* **1974**, *60*, 233−249.

(38) Hissung, A.; von Sonntag, C. *Int. J. Radiat. Biol.* **1979**, *35*, 449−458.

(39) (a) Barvian, M. R.; Greenberg, M. M. *J. Org. Chem.* **1995**, *60*, 1916−1917. (b) Barvian, M. R.; Greenberg, M. M. *J. Am. Chem. Soc.* **1995**, *117*, 8291−8292. (c) Greenberg, M. M.; Barvian, M. R.; Cook, G. P.; Goodman, B. K.; Matray, T. J.; Tronche, C.; Venkatesan, H. *J. Am. Chem. Soc.* **1997**, *119*, 1828−1839. (d) Kotera, M.; Bourdat, A.-G.; Defrancq, E.; Lhomme, J. *J. Am. Chem. Soc.* **1998**, *120*, 11810−11811.

(40) Gromova, M.; Balanzat, E.; Gervais, B.; Nardin, R.; Cadet, J. *Int. J. Radiat. Biol.* **1998**, *74*, 81−97.

Scheme 4

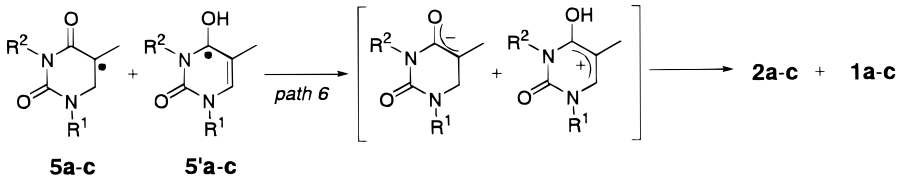

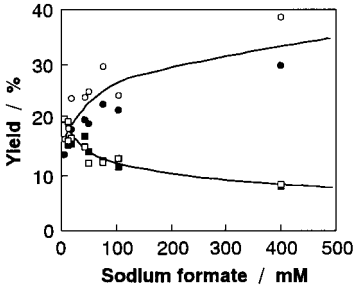

Figure 6. Variation of the yields of dihydrothymidines (●, **2c**[***S***]; ○, **2c**[***R***]) and C5−C5′-linked dihydrothymidine dimers (□, **3c**[***RS***]; ■, **3c**[***RR***] + **3c**[***SS***]) in the γ-irradiation (150 Gy) of Ar-purged phosphate buffer solutions (pH 7.0) of **1c** (0.1 mM) with increasing concentrations of sodium formate.

Radiolytic Reduction of N1-Substituted Thymine Derivatives. Aqueous solutions of N1-substituted thymine derivatives (**1a**−**c**; 5 mM) containing an excess amount (1 M) of sodium formate were prepared with water ion-exchanged using a Corning Mega-Pure System MP-190 (>16 MΩ cm). Typically, the pH of the aqueous solutions was adjusted to 7.0 ± 0.1 with phosphate buffer (2 mM). For the experiments on pH dependence of the radiolytic reduction, aqueous solutions of **1a**−**c** (1 mM) containing sodium formate (200 mM) or 2-methyl-2-propanol (100 mM) were buffered at pH 3−11 with phosphate buffer (2 mM) and sodium hydroxide. All the solutions were purged with Ar and irradiated in a sealed glass ampule at room temperature with a ^{60}Co γ-ray (dose rate: 0.89 Gy min^{-1}) or an X-ray source (5 Gy min^{-1}) (Rigaku RADIOFLEX-350).

HPLC. Aliquots (10 μL) of the irradiated solutions were analyzed by high-performance liquid chromatography (HPLC), using a Shimadzu 10A HPLC system equipped with a Rheodyne 7725 sample injector. Sample solutions were injected onto a reversed-phase column (Wakosil 5C18, ϕ 4.6 mm × 150 mm) containing C18 chemically bonded silica gel (5 μm particle size) for analysis of **3a**,**b**. The C5−C5′-linked dihydrothymidine dimers (**3c**) were analyzed using a reversed-phase column (Nacalai Cosmosil 5C18 MS, ϕ 4.6 mm × 250 mm). The phosphate buffer solutions (10 mM, pH 3.0) containing varying concentrations of methanol (10−25 vol %) were delivered as the mobile phase at a flow rate of 0.6 mL min^{-1}. The column eluents were monitored by the UV absorbance at 210 nm. For isolation of the products, the irradiated solutions were evaporated to a minimum volume and were subjected to preparative HPLC, using a Tosoh Preparative HPLC system equipped with a Chromatocorder 12 (System Instruments). The isolation was performed on a reversed-phase column (Wakosil 10C18, ϕ 10 mm × 300 mm) containing C18 chemically bonded silica gel (10 μm particle size), and phosphate buffer solution (10 mM, pH 3.0) containing 5−20 vol % methanol was delivered at a flow rate of 3 mL min^{-1}. After aqueous fractions of the respective products were collected automatically and evaporated, the resulting residues were lyophilized and subjected to spectroscopic measurements.

Spectroscopic Measurements. ^{1}H and ^{13}C NMR spectra were recorded on a JEOL GSX-270 (270 MHz) or EX-400 (400 MHz) Fourier transform NMR spectrometer. The C5−C5′-linked dimers produced from thymidine were measured in D_2O with reference to 3-(trimethylsilyl)propionic-2,2,3,3-d_4 acid (TSP) sodium salt (Aldrich) using EX-400, and those from 1-methylthymine and 1,3-dimethylthymine in dimethyl sulfoxide-d_6 (Nacalai Tesque) were measured using GSX-270. Chemical shifts in DMSO-d_6 were expressed from the residual proton signals of DMSO (δ = 2.49 ppm) for ^{1}H NMR and from the carbon signals (δ = 39.50 ppm) for ^{13}C NMR, respectively. High-resolution positive FAB mass spectra (FAB−HRMS) were recorded on a JEOL JMS-SX102A spectrometer, using glycerol matrix: 5,5′-bi-5,6-dihydro-1-methylthymines calcd for $C_{12}H_{18}N_4O_4$ 283.141 $(M + H)^+$, found 283.142 (**3a**[***meso***]) and 283.143 (**3a**[***rac***]); 5,5′-bi-5,6-dihydro-1,3-dimethylthymines calcd for $C_{14}H_{22}N_4O_4$ 311.172, found 311.173 (**3b**[***meso***]) and 311.173 (**3b**[***rac***]); 5,5′-bi-5,6-dihydrothymidines calcd for $C_{20}H_{30}N_4O_{10}$ 487.204, found 487.204 (**3c**[***RS***]), 487.206, and 487.206 (**3c**[***RR***] and **3c**[***SS***]).

X-ray Crystallography. The colorless needle-shaped crystals of C5−C5′-linked dihydrothymine dimers were grown from aqueous solutions (~3 mg mL^{-1}). While the dihydrothymidine dimers were coated with 40 vol % collodion-ethanol solution, the other dihydrothymine dimers were mounted directly on a glass fiber. All measurements were made on a Rigaku AFC7R diffractometer with graphite-monochromated Mo−Kα radiation (λ = 0.71609 Å) and a 12-kW rotating anode generator. The diffraction data were collected at room temperature using the $\omega - 2\theta$ scan mode to a maximum 2θ value of 60.0° for **3a**[***meso***] and **3a**[***rac***], 55.1° for **3b**[***meso***], and 55.0° for **3b**[***rac***] and **3c**[***RS***]. The intensities of three representative reflections that were measured after every 150 reflections remained constant throughout the data collection, indicating electronic stability of the sample crystals except for **3c**[***RS***]. The structures were solved by direct methods (SHELXS 86,[41] SIR 88[42]) and expanded using a Fourier technique. The positions of the hydrogen atoms were calculated. While hydrogen atoms of **3a**[***meso***] were refined isotropically, only isotropic *B* values were refined for hydrogen atoms of the other dimers.

Acknowledgment. This work was supported by Grants-in-Aid for JSPS Fellows (No. 00086200) and for Scientific Research (C) (No. 09640632) from the Ministry of Education, Science, Sports, and Culture of Japan. We are grateful to Dr. Tôru Ueno for performing fast atom bombardment mass spectral analysis.

Supporting Information Available: Copies of ^{1}H NMR and ^{13}C NMR spectra and X-ray crystallographic data of **3a**,**b**[***meso***], **3a**,**b**[***rac***], **3c**[***RS***], **3c**[***RR***], and **3c**[***SS***] (except for X-ray structural data of **3c**[***RR***] and **3c**[***SS***]). This material is available free of charge via the Internet at http://pubs.acs.org.

JO990059S

(41) Sheldrick, G. M. In *Crystallographic Computing 3*; Sheldrick, G. M., Kruger, C., Goddard, R., Eds.; Oxford University Press: Oxford, 1985; pp 175−189.

(42) Burla, M. C.; Camalli, M.; Cascarano, G.; Giacovazzo, C.; Polidori, G.; Spagna, R.; Viterbo, D. *J. Appl. Crystallogr.* **1989**, *22*, 289−303.